

## Density Measurement of Powdery and Porous Substances with a Gravimetric BET Adsorption Apparatus

Han-Sung Kim, Hyun-Woo Cho, Kwang-Soon Lee<sup>†</sup>, and Woon-Sun Ahn\*

*Department of Chemistry, Sung Kyun Kwan University, Suwon 440-746*

<sup>†</sup>*Department of Chemistry, Song Sim College For Women, Buchon 422-743. Received April 21, 1992*

An accurate method of density measurement is proposed. The method makes use of a gravimetric adsorption apparatus and is quite suitable for powdery and porous solid samples. The sample volume is determined by measuring its buoyancy with microbalance and the mass is measured in vacuum in the absence of buoyancy effect. Densities of inorganic compounds, such as alumina and perovskite, and some organic compounds are determined with the proposed method, and the results are compared with the values either determined with conventional methods or obtained from literatures.

### Introduction

The density of material, a ratio of the sample mass to the volume, is one of the fundamental properties. However, the result of measurement is subjected to a considerable error especially when the sample is fine powdery or porous solid. The density of solid sample is commonly determined with a conventional liquid displacement method<sup>1-4</sup>, in which the real volume is measured by the volume of the liquid which is displaced by the sample. In most measurements, however, a considerable amount of gas dispersed as fine bubbles and trapped in fine capillary pores can not be readily displaced by the liquid, hence an overestimated value of the sample volume is resulted. This inaccuracy in the sample volume measurement combined with the buoyancy effect which comes in when the sample mass is measured in the air results in an inaccurate density. This inaccuracy is significant especially when the sample is fine powdery or fine porous solid. In the gas volume measuring method, the known mass of sample is placed in a known volume of container and the volume of an inert gas which fills the pores and the free space is measured to obtain the sample volume. This method is also subject to a considerable error due to the inherent inaccuracy in the gas volume measurement. X-ray data for lattice dimension is also used to calculate the density. A correction for the lattice defects is neglected usually in calculating the density.

This paper is a supplement to a note previously reported in this journal<sup>5</sup>. The theoretical basis of the proposed method is the same, but the method is described in detail with the insertion of experimental basis in order to show the reliability of the method. Variety of samples ranging from organic to inorganic compounds are used for density measurement, and the results are found very satisfactory.

### Experiments

**Samples.** Alumina samples are obtained by immersing aluminium foils with oxide film grown on it in an acid solution to dissolve off the metal. The oxide left thereupon is very fragile and porous, and is known to have an  $\gamma$ -alumina structure.

The perovskite-type mixed oxide samples are synthesized by the citrate precipitation method<sup>6</sup> from the metal nitrates

in this laboratory. The crystal structures of synthesized oxides are confirmed with SEM and XRD. Other organic and inorganic samples are commercially obtained reagent grades.

**Sensitivity of the balance.** A gravimetric adsorption apparatus with a Nernst-Donau type quartz beam microbalance is used<sup>7,8</sup>. It has been described in a previous paper<sup>8</sup>. The sensitivity of the microbalance is determined by counterbalancing the standard weight. Alnico wire is used as the counter weight around which magnetic field is generated by the controlled electric current passing through a solenoid, wound right around the outer wall of the encasing tube. Gold weights of known mass ranging from 372  $\mu\text{g}$  through 3183  $\mu\text{g}$  are used as standard weights for calibration of the balance. A good linearity between the voltage of the counterbalancing current and the mass of the standard weights was obtained. The sensitivity of the balance calculated from this linearity was 2.23  $\mu\text{g}/\text{mV}$ .

**Blank volume of the balance.** Whenever the mass of a sample is measured with a balance, there arises a buoyancy effect due to the unequal volume distribution between two arms of the balance beam. The magnitude of this buoyancy effect is a function of the pressure of the gas surrounding the balance according to the Archimedes' principle. It can be given by the following equation, assuming the ideal behavior of the gas.

$$W = -\frac{M\Delta V}{RT} P$$

where,  $M$  is the molar mass of the gas,  $\Delta V$  the volume difference between two arms of the balance beam, and other symbols have their usual physical meanings. The buoyancy is the difference in weights measured in the fluid and in vacuum. Argon is used as a fluid gas. The buoyancy is measured at various pressures and plotted against the pressure. A straight line should be resulted in according to the above equation, with the slope of  $M\Delta V/RT$ . From the slope  $\Delta V$  can be calculated.

The value of  $\Delta V$  determined in this way includes two contributions: one from the sample and the other from the unequal volume distribution of the balance between two arms. In order to estimate the latter effect, following experiments are carried out with the sample bucket loaded successively with 5 tiny glass bulbs of known volume. The chamber arm,

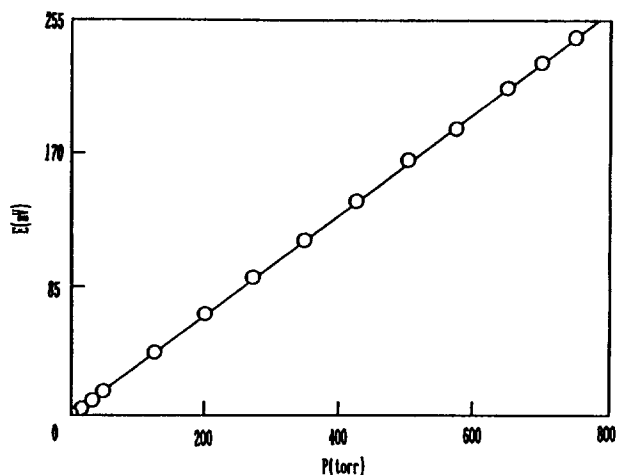


**Figure 1.** Buoyancy vs. the gas pressure, when the sample bucket is loaded with a glass bulb of 0.377 cm<sup>3</sup>.

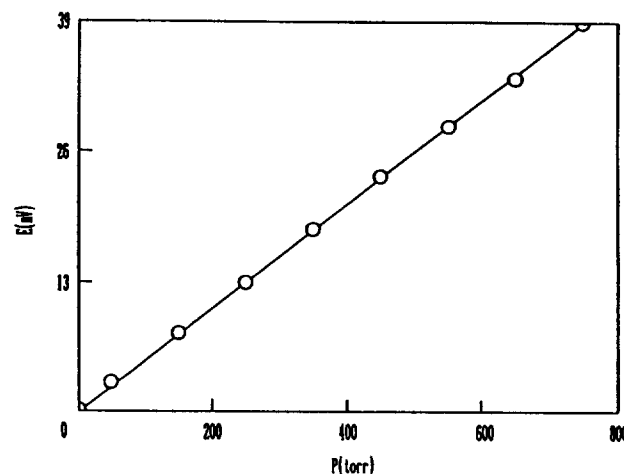


**Figure 2.** Buoyancy vs. the gas pressure, when the sample bucket is loaded with La<sub>0.97</sub>Sr<sub>0.03</sub>NiO<sub>3</sub>.

**Table 1.** Blank Volume of the Balance

Bulb	1	2	3	4	5
Volume of bulb (cm <sup>3</sup> )	0.377	0.378	0.388	0.440	0.567
$\Delta V$ (cm <sup>3</sup> )*	0.309	0.306	0.321	0.364	0.487
Blank volume	-0.068	-0.072	-0.067	-0.076	-0.080

\* Values are the volumes measured without blank volume correction.

inside of which the sample bucket is suspended, is immersed in ice water, and kept the temperature of the system at 0°C during the measurement. The displacing gas, argon, is introduced slowly through a variable leak valve (capable of controlling the inlet gas at the rate of 10<sup>-10</sup> cm<sup>3</sup>/sec through 100 cm<sup>3</sup>/sec). With a glass bulb of 0.377 cm<sup>3</sup> loaded on the sample bucket, the counterbalancing voltage is measured as a function of the gas pressure. The buoyancy is calculated and plotted against the gas pressure as shown in Figure 1. Similar measurements are repeated with other glass bulbs successively. These results are used to calculate the volume contribution of the balance itself. This contribution, shown in Table 1, is a blank volume to be corrected to the volume of the sample measured in the course of the density measurement. The blank volume obtained in this way is -0.073 cm<sup>3</sup> in average. The negative sign means that the counterweight side of the balance is bulkier.

## Results and Discussions

The sample mass is measured in vacuum in order to eliminate buoyancy and gas adsorption effects. For this purpose the mass of the sample is measured in air and the corresponding voltage which counterweight the sample is measured with the microbalance at first. Then the system with the sample loaded on the balance is evacuated down to 10<sup>-5</sup>-10<sup>-6</sup> torr. The counterweighing voltage is measured with the sample in this completely desorbed state. The difference between the voltage in air and in vacuum can be attributed to the elimination of the buoyancy and adsorption effects.

**Table 2.** The Densities Determined with Various Method

Sample	Density (g/cm <sup>3</sup> )			
	This	Conventional	Lattice parameter <sup>9</sup>	Literature <sup>10,11</sup>
LaNiO <sub>3</sub>	6.84	6.71	7.22	
La <sub>0.99</sub> Sr <sub>0.01</sub> NiO <sub>3</sub>	6.81			
La <sub>0.98</sub> Sr <sub>0.02</sub> NiO <sub>3</sub>	7.00	6.64		
La <sub>0.97</sub> Sr <sub>0.03</sub> NiO <sub>3</sub>	6.83			
La <sub>0.96</sub> Sr <sub>0.04</sub> NiO <sub>3</sub>	6.84	6.04		
La <sub>0.94</sub> Sr <sub>0.06</sub> NiO <sub>3</sub>	6.82			
La <sub>0.99</sub> Ba <sub>0.01</sub> NiO <sub>3</sub>	7.57			
LaFeO <sub>3</sub>	6.67	6.00	6.64	
Aluminium foil with oxide film (1)	2.98			
Aluminium foil with oxide film (2)	3.16			
$\gamma'$ -alumina (3)	2.56			
Mannitol (C <sub>6</sub> H <sub>14</sub> O <sub>6</sub> )	1.53			1.52
Thiourea (H <sub>2</sub> NCSNH <sub>2</sub> )	1.40			1.41
Anthracene (C <sub>14</sub> H <sub>10</sub> )	1.21			1.28
Si <sub>3</sub> N <sub>4</sub>	3.15			3.20
$\alpha$ -SiC	3.37			3.21
$\alpha$ -alumina	4.14			4.00
BaCO <sub>3</sub>	4.38			4.29
TiB <sub>2</sub>	4.69			4.50
TiN	5.45			5.21
NiO	6.74			6.67

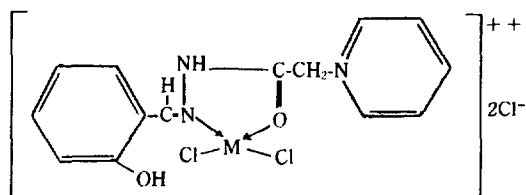
The mass equivalent of this voltage difference is calculated and subtracted from the mass in the air to obtain an accurate mass in vacuum.

The sample volume is determined from the buoyancy measured in the course of its mass measurement. The buoyancy effect measured for perovskite La<sub>0.97</sub>Sr<sub>0.03</sub>NiO<sub>3</sub> is shown in Figure 2. The effects of other samples are not shown as they give similar straight lines. The densities obtained from the masses and volumes measured in this way are

**Table 1.** Results of the Elemental Analysis of the Solid Complexes

Complex	C% Found	H% (Cal.)	N% (Cal.)	Molar con- ductance, $\lambda_m$
[Fe(L)] <sup>2+</sup> ·2Cl <sup>-</sup> ·4H <sub>2</sub> O	34.1 (34.3)	3.9 (4.3)	8.2 (8.6)	200
[Co(L)] <sup>2+</sup> ·2Cl <sup>-</sup> ·3H <sub>2</sub> O	35.7 (35.3)	4.6 (4.2)	8.6 (8.8)	—
[Cu(HL)] <sup>2+</sup> ·2Cl <sup>-</sup> ·4H <sub>2</sub> O	32.6 (33.1)	3.6 (4.1)	7.8 (8.3)	200
[Zn(HL) <sub>2</sub> ] <sup>4+</sup> ·4Cl <sup>-</sup>	46.7 (46.6)	3.9 (4.1)	11.6 (11.0)	415

The general structure of these complexes can be represented as follow<sup>6</sup>.

**Table 2.** Analysis of the TG Curve of the Cobalt Compound

Wt. loss, mg	$t_1$ min	$t_2$ °C	$dm$	$-dm/dt$ $=v$	Log $v$ (-)	$1/T \times 10^3$
3.9	51.1	199.0	15.7	0.307	0.512	1.80
7.9	60.0	331.2	11.7	0.195	0.709	1.65
9.8	68.0	375.1	9.8	0.144	0.841	1.54
11.8	72.7	400.7	7.8	0.107	0.969	1.48
15.6	87.9	484.9	4.0	0.045	1.341	1.31
17.3	97.2	536.1	2.3	0.024	1.625	1.23
19.3	104.2	574.6	0.3	0.0028	2.540	1.17

med by the analysis of the first step of the corresponding TG curve.

2. A sharp exothermic peak at 279.3°C which may be due to the lattice rearrangement.

3. An exothermic shoulder peak at 345.3°C is consistent with the melting of the complex.

4. A strong broad endothermic one at 438.9°C may be attributable to a result of the decomposition to the chelate bonds, leading to the formation of the final stable product "metal oxide".

**Analysis of the TG Curve.** Table 2 shows the weight loss of the cobalt complex with the time (or temperature) as one example for such analysis. In order to evaluate the kinetic parameters  $n$ ,  $E_a$  and  $A$  (they are order of the decomposition-process, the activation energy and the pre-exponential factor respectively), Chatterjee's method<sup>7</sup> was used. This method is based on the general equation for the rate of a heterogeneous kinetics,  $V$

$$V = -\frac{dm}{dt} = km^n \quad (1)$$

where  $k$ ,  $m$  and  $t$  are the rate constant of the reaction, the

**Table 3.** The Evaluated Kinetic and Thermodynamic Parameters of the Investigated Compounds

Compound	$n$	$E_a$ KJ/mol	log $A$	$\Delta H^\ddagger$ KJ/mol	$\Delta S^\ddagger$ KJ/mol/deg	$\Delta G^\ddagger$ KJ/mol
Fe-Complex	0.75	162.17	14.25	154.80	14.63	152.50
Co-Complex	0.87	240.73	12.21	231.90	15.17	215.60
Cu-Complex	0.80	193.60	13.81	179.76	14.92	168.13
Zn-Complex	0.92	154.55	12.93	138.45	17.86	129.27

active weight of the reacting material and the time elapsed from the start of the experiment respectively. Substituting  $k$  from the Arrhenius equation into the equation (1) gives:

$$\log V = \log A + n \log m - \frac{E_a}{2.303RT} \quad (2)$$

Plotting  $\log V$  versus  $1/T$  gives a straight line. Its slope equals to  $-E_a/2.30R$ , and its intercept is  $\log A + n \log m$ . From Table 3 it is clear that the order of the decomposition reaction ( $n$ ) for all complexes is nearly unity. This means that the mechanism of the decomposition processes for all the complexes studied is the same. The activation energy of the complexes decreases in the following order:

Cu(II) < Co(II) < Fe(III) < Zn(II)-complex. This variation of the activation energy increases with the increase of the strength of the (O→M←N) bond, and increases with the increase in the cation radius. This leads to a stronger attraction between the central metal ion and the hetero atoms of the bidentate ligand. It is expected that the thermal stability and the activation energy also decrease as follows: Cu(II) > Co(II) > Fe(III) > Zn(II)-complex. The experimental lower thermal stability in the case of the Cu(II) compound than the Co(II) complex may be attributed to the special electronic configuration of the Cu(II) as  $4s^1 3d^{10}$  which leads to shielding effect and hence decreases the attraction between the nucleus of the central metal ion and the hetero atoms of the ligand. This order of thermal stability of the complexes studied is in good agreement with the same arrangement for similar studies<sup>8,9</sup>.

**Analysis of the DSC Curves.** The DSC curves of all the complexes studied showed two different peaks. The first one is an exothermic peak with small intensity at low temperature, and the second peak was a big endothermic one at high temperature (above 450°K). The thermodynamic parameters  $\Delta H^\ddagger$ ,  $\Delta S^\ddagger$  and  $\Delta G^\ddagger$ , [which are the activation enthalpy, activation entropy, and free energy change for the thermal decomposition process, respectively], were evaluated using the normal methods<sup>10,11</sup>, and these values are given in Table 3. It is seemed from this table that all  $\Delta H^\ddagger$  values for the different complexes have positive values which indicate that the decomposition reactions are endothermic processes. The positive values of  $\Delta S^\ddagger$  for all complexes mean that the decomposition process is accompanied by the increase of the entropy change of the system due to the liberation of different fragments, and hence increases the disorder of the system. The positive values of  $\Delta G^\ddagger$  as seen from Table 3 indicates that the decomposition reactions for all the investigated compounds are not spontaneously occurred, and the higher value corresponds to the higher thermal sta-

bility. From the above analysis data, it is clear that the decomposition process takes place through the following four steps:

1. The decomposition of the pyridinium rest, the formation of Cl<sub>2</sub> gas, and pyridine molecule are related to the first exothermic peak in DTA curves.

2. Decomposition of (-CH=N) and the formation of the volatile salicylaldehyde are related to the second exothermic peak.

3. The degradation of (N-C) bond, and the evolution of N<sub>2</sub> and CO are indicated by the first endothermic peak.

4. The last step which corresponds to the rupture of the bonds between the metal ion and the hetero atoms of the bidentate ligand gives the characteristic endothermic peak in DTA curves. As a result of this step, volatile metal oxide is formed. The breaking of the last bond is responsible for the difference in the activation energy of the various investigated complexes.

This suggested mechanism is similar to our first one given in the literature<sup>12</sup>.

### References

1. J. Zsako, *J. Phys. Chem.*, **72**, 2406 (1968).

2. M. M. Abou Sekkina and M. G. Abou El Azm, *Thermochemi Acta*, **77**, 211 (1984).
3. B. F. Aycock, *J. Amer. Chem. Soc.*, **73**, 1351 (1951).
4. G. Vallebona, *J. Therm. Anal.*, **16**, 49 (1979).
5. K. Boguslawska, K. and A. Cygenski, *J. Therm Anal.*, **16**, 73 (1979).
6. F. T. M. Ibrahim, M. N. H. Moussa, A. M. Shalaby, and M. A. H. Hafez, *Egypt J. Chem.*, **19**(3), 527 (1976).
7. P. K. Chatterjee, *J. Polymer Sci.*, **3**, 4253 (1965).
8. B. Lakatos, J. Bohus, and Cy. Medgyesi, *Magy. Kem. Folyoirate*, **66**, 91 (1960).
9. K. Boguslawska and A. Cygensiki, *J. Therm. Anal.*, **16**, 73 (1979).
10. R. L. Bohon, Proceeding of the first Toronto Symposium on Thermal Analysis, Chemical Institute, Canada p. 63 (1965).
11. T. Ozawa, *Bull. Chem. Soc. Japan*, **39**, 2071 (1966).
12. M. E. M. Emam, M. A. H. Hafez, and M. N. H. Moussa, *J. Thermal. Anal.*, **32**, 945 (1987).

given in Table 2. The densities determined by the conventional method of liquid displacement, those calculated from lattice parameters<sup>9</sup> and the literature values<sup>10,11</sup> are also listed for comparison. The densities measured with the conventional liquid displacement method are found to give smaller values, as expected. Fairly good agreement is obtained in general between the values of the proposed method and those calculated from the lattice parameters<sup>9</sup>. Also, the values of this method agree very well with the literature values<sup>10,11</sup>. The proposed method is simple, intuitive, and yet gives quite an accurate result. This method will be especially of value when the sample is in powdery, porous form, or is reactive to displacing liquids.

**Acknowledgement.** This work is supported financially by the Ministry of Education, through the Basic Research Institute Program.

### References

1. V. R. Choudhary and S. H. Vaidya, *Research and Industry*, **26**, 1 (1981).
2. D. Geldart, *Chem. Eng. Sci.*, **34**, 155 (1979).
3. W. H. Salzberg, J. I. Morrow, S. R. Cohen, and M. E. Green, "Physical Chemistry Laboratory", Part I, Chapter 8, Macmillan Publishing Co., Inc., New York, 1978.
4. S. Lowell and Joan E. Shields, "Powder Surface Area and Porosity", Chapter 21, Chapman and Hall, New York, 1984.
5. W. Ahn, K. Lee, H. Cho, and J. Kim, *Bull. Korean Chem. Soc.*, **11**, 572 (1990).
6. D. J. Anderton and F. R. Sale, *Powder Metallurgy*, No. 1, 14 (1979).
7. S. P. Wolsky and E. J. Zdanuk, "Ultra Micro Weight Determination in Controlled Environments", Interscience Publishers, 1969.
8. W. Ahn, E. Yoo, H. Cho, and J. Kim, *Bull. Korean Chem. Soc.*, **9**, 244 (1988).
9. T. Nakamura, G. Petzow, and L. J. Gauckler, *Mat. Res. Bull.*, **14**, 649 (1979).
10. J. A. Dean, "Lange's Handbook in Chemistry", 12th Ed., McGraw-Hill, 1979.
11. S. Budaveri *et al.*, "The Merck Index", 11th Ed., MERCK & CO., INC., 1989.

## Thermochemical Behaviour of Some Salicylaldehyde G-P Complexes of Fe (III), Co (II), Cu (II) and Zn (II)

M. A. H. Hafez\* and M. N. H. Moussa

*Department Chemistry, Faculty of Science, Mansoura University, Mansoura, Egypt*

*Received May 15, 1991*

Through two different techniques TGA and DSC the thermal decomposition processes of salicylaldehyde G-P complexes having the general formula:  $[MCl_2(L)_2]^{2+} 2Cl^-$ ; where L=salicylaldehyde carbohydrazone pyridinium cation, and M=Fe (III), Co (II), Cu (II) and Zn (II), have been studied. From the obtained thermogravimetric curves the following parameters  $n$ ,  $E_a$ ,  $A$ ,  $\Delta S^\ddagger$ ,  $\Delta H^\ddagger$  and  $\Delta G^\ddagger$  were evaluated. The effect of the nature of the metal ions present in the complexes studied upon the calculated thermodynamic parameters was reported. A suitable mechanism for the thermal decomposition process was suggested.

### Introduction

The thermal behaviour of the complexes plays a very important role for chemist to understand the mechanism of the thermal process. This thermal behaviour is based on the qualitative and quantitative analysis of the DTA and TG curves respectively<sup>1-5</sup>. The aim of the present work is to describe the thermochemical behaviour of some complexes, discuss the differences in their thermal stabilities and also to find a suitable mechanism for the thermal decomposition process.

### Experimental

Syntheses of the complexes studied were carried out as

mentioned previously<sup>6</sup>. The stoichiometry of the solid compounds obtained was confirmed by the results of the elemental analysis, molar conductance of solution of the complex (see Table 1), and magnetic measurements.

The thermal decomposition has been studied in a Pt crucible by thermo-analyser [TGA-DTA (1600°C) GDTA 15, Setram Lyon-France and DSC 777 Lyon-France] using linear temperature programmer with a constant heating rate of 5 °C/min. Sample weight used was in the range of 20-37.2 mg.

### Results and Discussion

**Analysis of the DTA Curves.** All the DTA curves obtained showed four different peaks. For example, in the case of the cobalt-complex the following peaks were observed:

1. A sharp endothermic peak at 254.3°C which corresponds to the dechlorination of the chloride ions. This was confir-

\*To whom all correspondence should be addressed.